16th World Conference on Earthquake Engineering, 16WCEE 2017

Santiago Chile, January 9th to 13th 2017

Paper N° 3631

Registration Code: S-B1464939158

THE OCTOBER 1980 EL-ASNAM EARTHQUAKE IN N.W. ALGERIA: MODELLING INCOHERENCE OF GROUND MOTION

K. AfifChaouch[(1)], B. Tiliouine[(2)], M. Hammoutene[(3)], R. Rupakhety[(4)], S. Ólafsson[(5)]

[(1)] *Phd student, Ecole Polytechnique d'Architecture et d'Urbanisme, Algiers, Algeria, e-mail:karim.afifchaouch@gmail.com*

[(2)] *Professor, National Polytechnic School, LGSDS, Seismic Engineering and Structural Dynamics Laboratory, Algiers, Algeria, e-mail:tiliouine_b@yahoo.fr*

[(3)] *Professor, National Polytechnic School, LGSDS, Seismic Engineering and Structural Dynamics Laboratory, Algiers, Algeria, e-mail:hammoutene_m@yahoo.fr*

[(4)] *Professor, Earthquake Engineering Research Centre of the University of Iceland, Selfoss, Iceland, e-mail:rajesh@hi.is*

[(5)] *Professor and Director, Earthquake Engineering Research Centre of the University of Iceland, Selfoss, Iceland, e-mail:simon@hi.is*

Abstract

The main objective of this paper is to provide estimates of coherency functions of strong ground motion at engineering bedrock within the El-Asnam region (North-West Algeria). Due to lack of recorded array data, the so-called Empirical Green's Function (EGF) method is used to simulate ground acceleration at different points in the engineering bedrock of the study area. The event being simulated is the 10 October 1980, Ms 7.2 El-Asnam Earthquake. Ground motion recorded at the Sogedia factory station during the 8 November 1980 aftershock with local magnitude 5.6 was used as empirical Green's function. Lagged coherency functions estimated from simulated motions indicate significant loss of coherence with increasing frequency and separation distance. Since the EGF method, when used with Green's function at a single station, can primarily model source effects, which are interpreted as the main reason behind the observed loss of coherency. The results also indicate that source effects are the main source of ground-motion incoherence in the near-source area, whereas it is negligible in the far field.

In order to parametrize the estimated lagged coherency functions, they were compared with different models proposed in the literature. Curve fitting using nonlinear least square regression was performed to estimate the parameters of such models. It was found that the Hindy and Novak [1] model provides the best fit to the estimated lagged coherency functions. Along with the model parameters estimated in this study, this model, provides, at least, a first approximation, and possibly, an upper bound of ground motion incoherence in the study area for earthquake scenarios of the type presented in this study.

.

Keywords: Coherency function; spatial variability; strong ground motion; Green's function; El-Asnam Earthquake

1. INTRODUCTION

Lifelines systems experience differential movement of their supports during earthquakes. This differential motion of the supports may result in additional strains (or stresses) in their structural elements, which can, in the event of strong shaking, result in damage to the elements of the such structures (e.g., Walling and Abrahamson [2]). Attenuation effect results in reduction of ground motion amplitudes with distance from the source. At a local spatial scale, for example within a few hundred meters, attenuation effect is not critical, and spatial variation is due to physical processes such as (1) wave passage effects; (2) incoherence effects, which are due to multiple reflections and refractions of seismic waves in inhomogeneous medium, as well as complex superposition of waves radiated from different parts of the source; and (3) local site effects.

Engineering models of ground-motion incoherence are often deduced from strong-motion array data recorded during past earthquakes. Several models of coherency and correlation functions, both theoretical and empirical, are reported in the literature (see, for example, Harichandran and Vanmarcke [3]; Luco and Wong [4]). Such models are needed in simulating time series of spatially variable ground motion which are required in seismic response analysis of horizontally extended structures. It is well known that coherency functions are characteristic of local site, source, and wave propagation path. Therefore, models calibrated for a region may not be suitable for use in other areas (Somerville et al. [5]; Abrahamson et al. [6]; Santa-Cruz et al. [7]; Ding et al. [8]). Despite this, due mainly to lack of local data, coherency models calibrated for one region are often used to simulate ground motion in other regions. An alternative method of calibrating incoherence models is to numerically simulate spatially variable ground motion.

In this contribution, the numerical simulation technique known as Empirical Green's Function (EGF) Method, proposed first by Irikura et al. [9], is used to simulate ground-motion field at the bedrock of the El-Asnam area. The event being simulated is the 10 October 1980 Ms 7.2 El-Asnam Earthquake, while empirical Green's function is obtained from the ground motion recorded at Sogedia station during a local magnitude 5.6 aftershock. Ground motion simulated at stations with varying separation distance (up to 500m) are used to estimate lagged coherency functions. Models presented in Hindy and Novak [1], Luco and Wong [4] and Somerville et al. [5] are used to parametrize the estimated lagged coherency functions.

We present a brief summary of the concepts and terminologies related to stochastic estimation and empirical modelling of ground-motion incoherence, followed by the important equations and parameters used for numerical simulation of ground motion using the EGF method. Some samples of simulated ground motion are then presented along with lagged coherency functions estimated from them. Parametric modelling of the estimated coherency functions is then presented.

2. STOCHASTIC AND EMPIRICAL COHERENCY MODELS

Considering motions at two discrete locations i and j separated by a distance ξ, the complex coherency function in space and circular frequency (ω) is defined as:

$$\gamma_{ij}(\xi,\omega)=\frac{S_{ij}(\xi,\omega)}{\sqrt{S_{ii}(\omega)S_{jj}(\omega)}} \tag{1}$$

where $S_{ij}(\xi,\omega)$ is the smoothed cross spectral density function; and $S_{ii}(\omega)$ and $S_{jj}(\omega)$ are their smoothed power spectral density functions. Separating $\gamma_{ij}(\xi,\omega)$ into its absolute value and phase, we obtain

$$\gamma_{ij}(\xi,\omega)=\left|\gamma_{ij}(\xi,\omega)\right|\exp\left[i\theta_{ij}(\xi,\omega)\right] \tag{2}$$

where $0\leq\left|\gamma_{ij}(\xi,\omega)\right|\leq 1$, is the lagged coherency function and $\theta_{ij}(\xi,\omega)$ is phase spectrum.

Lagged coherency squared is termed as coherency. Generally, lagged coherency decreases with increase in separation distance and frequency. In this study, all coherencies are computed from simulated time series of ground acceleration; the simulation method is described in the following sections. The simulated time series are aligned to remove wave passage effects (see, for example, Ancheta et al. [10]). The stationary part of aligned time series is extracted by visual inspection of the time evolution of Arias Intensity of the simulated time series. A Tukey window with tapering length of 15% of the length of stationary part of the signal was applied. The windowed signals are then used to estimate power and cross spectral density functions which are smoothed. We smooth all power spectra using a Hamming spectral window with parameter of $M=39$ ($2M+1$ is the width of the window). This level of smoothing is selected in order to reduce the variance in lagged coherency.

Based on coherency estimated from recorded strong motion array data, several parametric coherency models have been proposed in the literature. In the present study, the models of Hindy and Novak [1], Luco and Wong [4] and Somerville et al. [5] are considered. Hindy and Novak [1] proposed the following model:

$$\left|\gamma(\xi,\omega)\right|=\exp\left[-(\alpha\omega\xi)^{\beta}\right] \tag{3}$$

where α and β are model parameters. The dimensionless parameter α is defined as $\alpha=\eta/v_s$, with $\eta=\mu\left(R/r_0\right)^{1/2}$, where v_s is the shear-wave velocity, R is the distance travelled by the wave, r_o the scale length of random inhomogeneities along the path, and μ^2 a measure of the relative variation of the elastic properties in medium. The semi-empirical model of Luco and Wong [4] is a particular case of (3) with $\beta=2$.

The model has been used extensively by researchers in seismic response analysis of lifelines (e.g. Luco and Wong [4]; Der Kiureghian and Neuenhofer [11]). The model is based on shear wave propagation through random media, an approximation which may be valid for the propagation of the waves from the source to the ground surface or from the source to the bedrock-layer interface. Zerva and Harada [12] have also used this model for the description of coherency of bedrock motion. Somerville et al. [5] proposed the following model which results in faster decrease of lagged coherency with frequency than with separation distance

$$\left|\gamma(\xi,\omega)\right|=\exp\left[-(a+b\omega^2)\xi\right] \tag{4}$$

where a and b are two independent constants.

3. EMPIRICAL GREEN'S FUNCTION METHOD

The empirical Green's function (EGF) method of Irikura et al. [9] considers a rectangular fault plane (length L, width W) divided into $l \times m$ elementary rectangular sub-faults on its surface. Denoting the Green's function associated with a sub-fault (i_o, j_o) by $u_{e_{i_o j_o}}(\mathbf{x},t)$, the total synthetic signal $U(\mathbf{x},t)$ at point $\mathbf{x}$ is given by:

$$U(\mathbf{x},t)=\sum_{i=1}^{l}\sum_{j=1}^{m}\frac{R_s(\theta_{ij},\varphi_{ij})r_{i_o j_o}}{R_s(\theta_{i_o j_o},\varphi_{i_o j_o})r_{ij}}F(t)*cu_{e_{i_o j_o}}(\mathbf{x},t) \tag{5}$$

where $*$ denotes convolution. The function $F(t)$ is given by:

$$F(t)=\delta(t-t_{ij})+\left(\frac{1}{n'}\right)\{1-\exp(-1)\}\sum_{k=1}^{(n-1)n'}\left[\exp\left\{\frac{-(k-1)}{(n-1)n'}\right\}\right]\times\delta\left(t-t_{ij}-\frac{(k-1)\tau}{(n-1)n'}\right) \tag{6}$$

and t_{ij} is given by Eq. (7):

$$t_{ij}=\frac{r_{ij}-r_o}{v_s}+\frac{\xi_{ij}}{v_r} \tag{7}$$

In these equations, t_{ij} is the phase delay, R_s is the radiation pattern (Aki and Richards[13]), τ is the rise time of event for which ground motion is being simulated, $r_{i_o j_o}$ is the Euclidean distance between the receiver $\mathbf{x}$ and the rupture starting point on elementary sub-fault (i_o, j_o), r_{ij} is the Euclidean distance between the receiver and the centre of the sub-fault (i, j), ξ_{ij} is the distance between the hypocentre and the centre of the sub-fault (i, j), v_s is the shear wave velocity, $v_r = 0.72 v_s$ is the rupture velocity, n' is an integer to eliminate spurious periodicity (Irikura [14]), $F(t)$ is the slip-time filtering function, c is the stress drop ratio, r_0 is the Euclidean distance between hypocentre and the receiver, and $\delta(t-t_{ij})$ represents Dirac delta function. The parameters l, m, and n are determined from the scaling relations given by Kanamori and Anderson [15]. For instance, when the seismic moment ratio of target earthquake (the one being simulated) to the elementary one (the one used for empirical Green's function) is N^3, the parameters l, m, and n should each one be equal to N (Irikura [14]); the total number of divisions along the length or the width of the fault so that the dimensions of sub-faults are small enough to be treated as point source.

Kamae et al. [16] revised the Kanamori and Anderson [15] relation to allow for the potential difference in stress drop between the target and the small event. The revised relations are:

$$\frac{L}{L_e}=\frac{W}{W_e}=\frac{D}{cD_e}=\frac{\tau}{\tau_e}=\left(\frac{M_0}{cM_{0_e}}\right)^{1/3}=N \tag{8}$$

where L and L_e are fault lengths, W and W_e are widths, τ and τ_e are rise times, and D and D_e are average slip, corresponding to the target event and small event, respectively. The rise time of the mainshock can be given from the similarity relation (Eq. 8) by using a small event rise time determined by picking the frequency of the significant trough of its Fourier spectra. For an objective estimation of the required parameters N and c, a spectral fitting procedure is used (see, for example, AfifChaouch et al. [17]).

4. RESULTS AND DISCUSSIONS

The EGF method, which has been widely used in simulating ground motion at a single location, is extended here to synthesize spatially varying horizontal ground motion at bedrock. The seismic scenario considered is the 10 October 1980 El-Asnam Earthquake of magnitude $M_s = 7.3$, for which ground motion records are not available. The earthquake occurred at 12:25 GMT and the hypocentre was estimated to be at 36°17'N, 1°41'E and at a depth of 12 km (Cisternas et al. [18]). The ground motion from the $M_L = 5.6$ aftershock of 08 November 1980 recorded at the Sogedia Factory Station is used as the empirical Green's function. The epicentral distance of this station is about 5 km. The aftershock event took place in the same rupture zone as the mainshock (target) event and with a similar faulting mechanism (Cisternas et al. [18]).

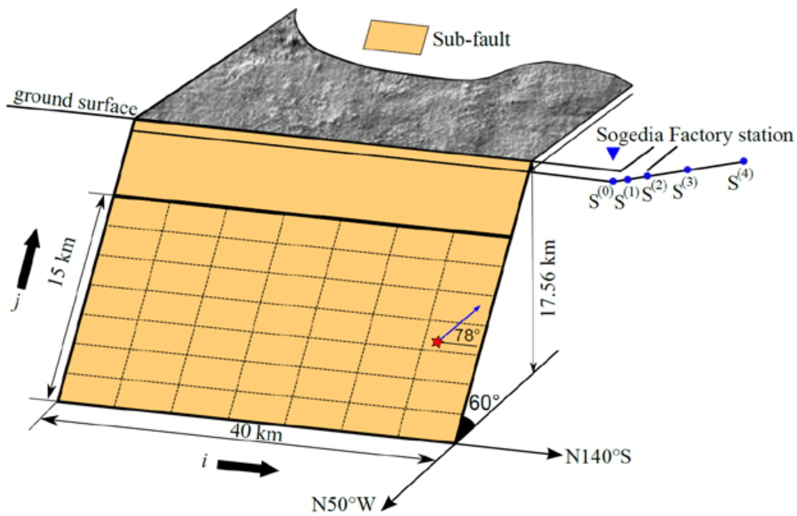

Fig. 1 – Schematic representation of the finite-fault model corresponding to the 1980 El-Asnam mainshock. The hypocenter is indicated by the red star, and the blue dots represent the locations of bedrock stations at which ground motion is simulated. Dimensions are not in scale (from AfifChaouch et al [17]).

In order to simulate ground motion at bedrock, the empirical Green's function should also correspond to the bedrock. Since the bedrock is not outcropping at the recording station, deconvoluted motion (Petrovski and Milutinovic [19]) corresponding to the bedrock, shown in Fig. 2a, is utilized. The time series of the deconvoluted motion is baseline corrected using the method described in Rupakhety et al. [20]. The fault plane is assumed to be 40 km x 15 km with a dip angle of 60° (see Fig. 1). Shear wave velocity is taken as 2 km/s (Yielding et al. [21]) and the corresponding rupture velocity (v_r) is equal to 1.44 km/s. The stress drop of the mainshock is 100 bars (from Dechamps et al. [22]) and, for the small event, a value of 82.57 bars is calculated by using the relation given by Boore [23] and a corner frequency of 0.37 Hz. This gives a stress drop ratio (c) equal to 1.21. The fault plane is divided equally into seven parts in both directions, i.e., the scale factor parameter N is equal to 7, and the number n' is taken as 20. The rise time of the small event is taken $\tau_e = 0.2$ sec; and that of the mainshock is $\tau = 1.4$ sec. The latter value is close to the 1s adopted by Dechamps et al. [22]. Other relevant parameters used in the simulation are given in AfifChaouch et al. [17]. The location of the hypocentre is shown with a red star in Fig. 1, and it lies on cell $(i_0, j_0) = (7,4)$ from where the rupture is assumed to propagate radially. Horizontal components of ground acceleration are then simulated at five stations at bedrock, namely $S^{(0)}$, $S^{(1)}$, $S^{(2)}$, $S^{(3)}$ and $S^{(4)}$ (see Fig. 1). Station $S^{(0)}$ is considered as the reference station and it lies directly under the Sogedia Factory station; the other stations are separated from it by 40 m, 100 m, 200 m, and 500 m. Epicentral distance of the reference station is 5 km. Ground acceleration time series simulated at the five stations are shown in Fig. 2b. Peak ground acceleration (PGA) of the simulated motion is close to 60% of acceleration due to gravity.

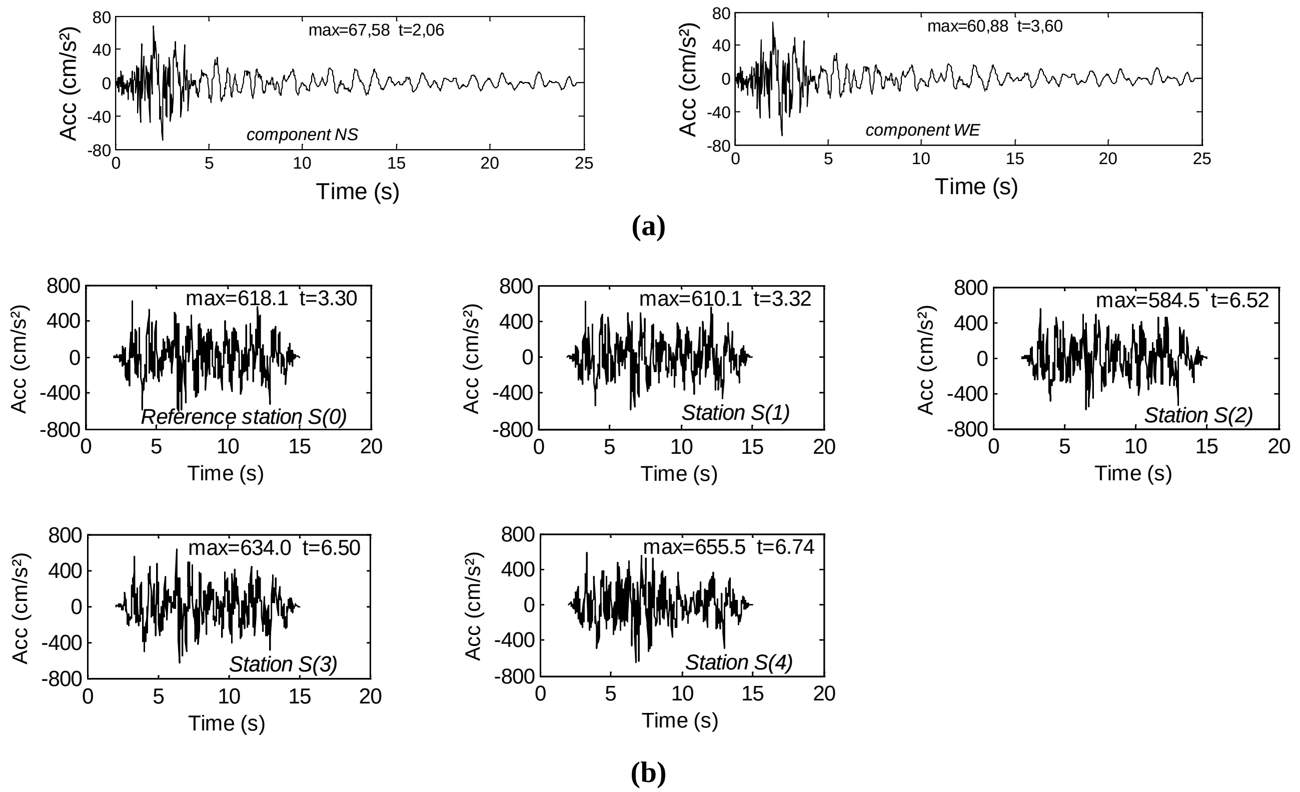

Fig. 2 – **(a)** Acceleration of bedrock (NS and WE component) obtained by deconvolution of ground acceleration due to the 8 November 1980 aftershock recorded at the Sogedia Factory station. The acceleration time series are obtained from Petrovski and Milutinovic (1981) [19]. **(b)** Ground-acceleration time series simulated at the 5 stations as indicated in the plots. Transverse component of motion is shown.

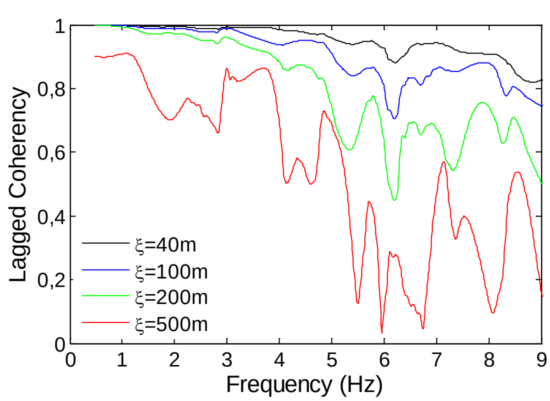

Fig. 3 – Lagged coherency functions computed from the time series shown in Fig. 2b.

Lagged coherencies computed from the simulated signals are shown in Fig. 3. The characteristics of the simulated lagged coherencies are similar to that estimated from strong-motion array data reported in the literature (see, for example, Zerva [24]). As expected, lagged coherency decays with increasing frequency and separation distance. It is noted that the coherency estimate for a separation distance of 500m first decreases with frequency, then starts increasing around 7 Hz. Such apparent increase of coherency with frequency is most likely due to uncertainties in the spectral estimation and smoothing operation (see Zerva [24] and Rupakhety and Sigbjörnsson [25]).

The coherency is significantly less than 1.0 at low frequencies (1-2 Hz) for the long station separation of 500 m and at intermediate frequencies (3-5 Hz) for the medium separation distance of 200 m. Since scattering effects are not modelled by the EGF when the Green's function is available at only one station, the relatively small value of coherence at low frequencies and large separate distance may be due to source effects in the near field, which has been reported to be prominent at low frequencies [6]. The results of simulation indicate that source effects in coherency are significant, considerable loss in coherency is obtained just by modelling the source effect. On the other hand, the source effects, site effects, and scattering effects may constructively and destructively interfere in coherency decay, and therefore to isolate these different effects from recorded data is not straightforward.

4.1 Parametric modelling of lagged coherency

In this section, we calibrate the three selected parametric models (see Section 2) to the coherency functions computed from simulated ground motion corresponding to the 1980 El-Esnam Earthquake. We note that we tried to fit to the simulated results, the model of Harichandran and Vanmarcke [3] without success, as this model did not seem to be well constrained by the simulated coherency data.

To calibrate the parameters of the models, we use non-linear least squares regression in the hyperbolic arctangent $\left(\tanh^{-1}\right)$ transformation of lagged coherency. Such a transformation is preferable because the transformed variable has approximately frequency independent variance (see, Jenkins and Watts, [26]). The frequency and separation distance ranges used in fitting the model were $\left[0-8\right]$ Hz and $\left[0-500\right]$ m, respectively. The regression parameters found to be for the Hindy and Novak [1] model $\alpha = 5.87\times10^{-5}$ and $\beta = 1.52$. The R-squared value of the fit was found to be 0.88 with a root mean square error RMSE of 0.30. For the Luco and Wong model $\alpha = 9.41\times10^{-5}$, R-squared=0.82 and RMSE=0.38 and for the Somerville model $a = 7.42\times10^{-6}$, $b = 1.03\times10^{-6}$, R-squared=0.89 and RMSE=0.29.

The comparison of the fitted models with the lagged coherency of simulated ground motion is presented in Fig. 4 for four different separation distances, as indicated in the plots of the figure. The comparison shows that the Hindy and Novak [1] and Somerville et al. [5] models are flexible and fit the data well for the four separations distance. At 500m the Hindy and Novak [1] model fit better in low frequency 0-2 Hz. than the Sormerville et al. model [5]. The Luco and Wong [4] model fits the simulated lagged coherencies relatively well for separation distance up to 100 m. For separation distance of 200 m, the fit is good up to a frequency of 6 Hz. For separation distance of 500 m, it falls and differs significantly from the estimated coherency function except at the low frequency up to 2Hz. The quality of fit is also clear from the residuals (difference between model prediction and simulated results) in $\tanh^{-1}$ transformation as shown in Fig. 5. The mean value of the residuals is generally close to 0, while it is clearly most biased for a separation distance of 500 m and the Luco and Wong [4] model.

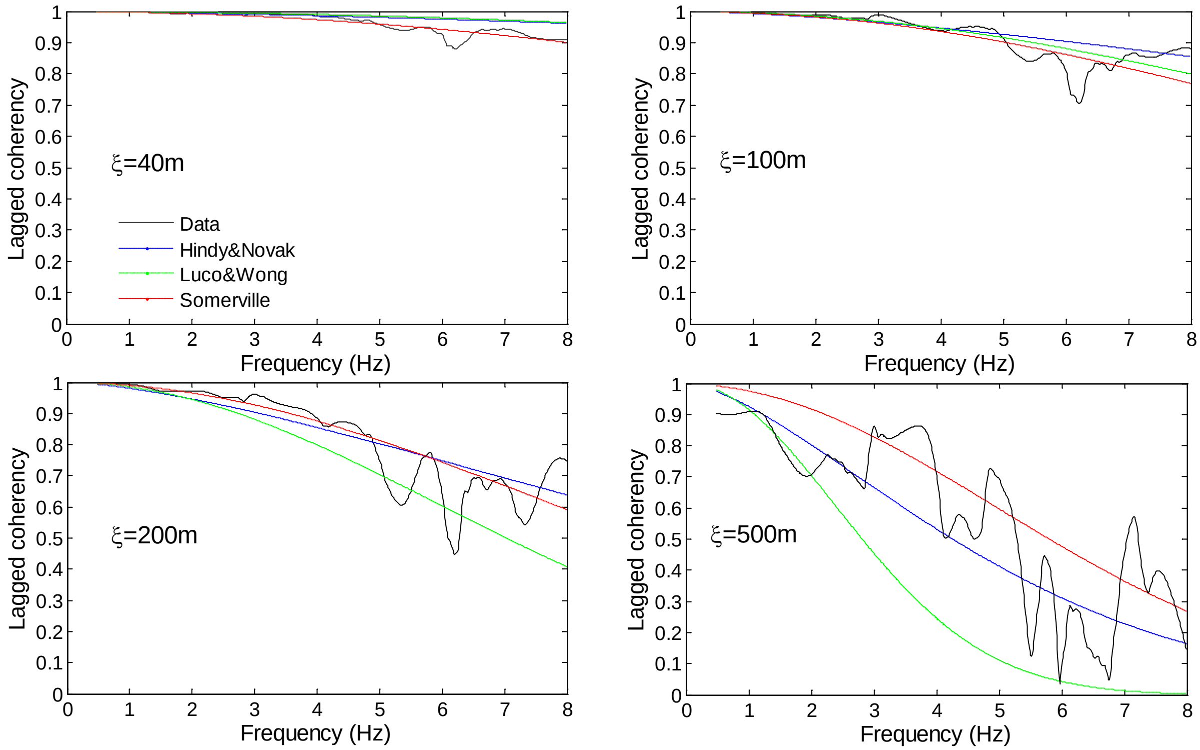

Fig. 4 – Comparison of three parametric models to the lagged coherency obtained from simulated ground acceleration field.

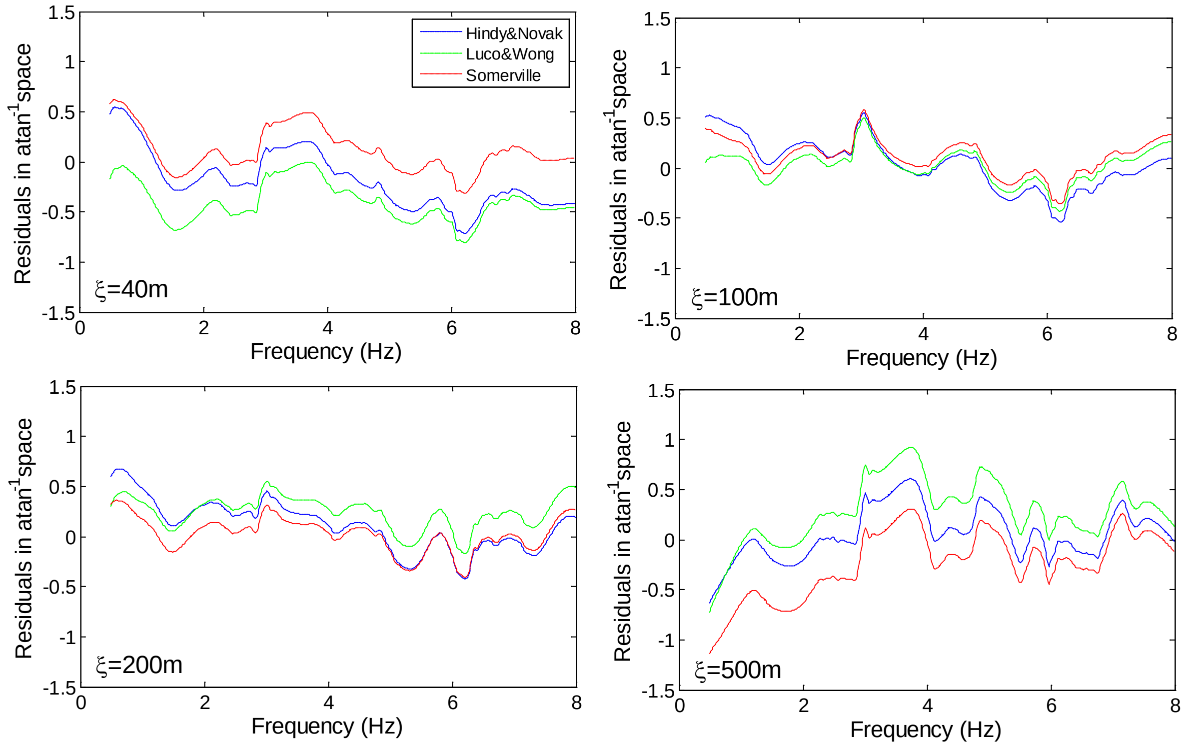

Fig. 5 – Residuals (in $\tanh^{-1}$ transformation) between the simulated lagged coherencies and the parametric models fitted to them (see Fig. 4).

5. CONCLUSIONS

The main contribution of this work is to present an approach to simulate spatially variable ground motion using the empirical green function method. This method has been extensively used in the literature to simulate point estimates of strong ground motion. In this work, we test whether it is suitable to simulate ground motion field within a relatively small spatial extend, thereby modelling incoherence effects. The case study and parametric study presented herein suggest that the presented approach is suitable of simulating incoherence due to finite source effect. In particular, plane wave coherency estimates can be obtained through such simulations. Although, loss in coherency is due to source, scattering, and local site effects, the present methodology captures only the effect of finite source. This is a limitation of the method. Nevertheless, in absence of recorded data, the method can be useful in modelling spatially variable ground motion, to the extent that the simulated coherencies can be considered as upper bounds of what is expected in presence of scattering and local site effects.

Further research in incorporating scattering and local site effects in simulated lagged coherencies is underway. Of special interest here is the development of models to convert lagged coherencies at bedrock to those at surface of a random soil layer. In addition, investigation of scattering effects will also be valuable. In the practical sense, and in absence of strong motion array data in the study region, the results presented herein could provide a rough approximation of ground motion coherency, which can be used in (a) random vibration analysis of lifeline structures, or (b) simulating spatially variable ground motion for time history analysis of such structures. To facilitate such modelling, parametric models of lagged coherency have been calibrated. Based on an extensive testing of many available models, the model of Hindy and Novak [1] is found to be the most suitable one for the study area.

6. REFERENCES

[1] Hindy A, Novak M (1980): Pipeline response to random ground motion. *Journal of Engineering Mechanics*, ASCE, 106 (2): 339-360.

[2] Walling M, Abrahamson N (2007): Spatial coherency of ground motions for embedded structures. *4th International Conference on Earthquake Geotechnical Engineering*, Thessaloniki, Greece.

[3] Harichandran RS, Vanmarcke E (1986): Stochastic variation of earthquake ground motion in space and time. *Journal of Engineering Mechanics*, *ASCE* 112(2): 914-925

[4] Luco JE, Wong HL (1986): Response of a rigid foundation to a spatially random ground motion. *Earth. Eng. Struc. Dyn*14: 891-908

[5] Somerville PG, McLaren JP, Saikia CK (1988): Site-specific estimation of spatial incoherence of strong ground motion. *Proc. Earth. Engin. Soil Dyn. II, Recent Advances in Ground-Motion Evaluation, ASCE*, Park City, Utah, 188-202

[6] Abrahamson N, Schneider JF, Stepp JC (1991): Spatial coherency of shear waves from the Lotung, Taiwan large-scale seismic test. *Structural Safety* 10: 145-162

[7] Santa-Cruz S, Heredia-Zavoni E, Harichandran RS (2000): Low-frequency behaviour of coherency for strong ground motions in Mexico City and Japan. *12th World Conference in Earthquake Engineering*, Auckland, New-Zealand, Paper No.76:1-8

[8] Ding H, Liu Q, Jin X, Yuan Y (2004): Coherency function model of ground motion at base-rock. In Proc. *14th World Conference Earthquake Engineering*, Paper No.2692 Vancouver, B.C., Canada

[9] Irikura K, Kagawa T, Sekiguchi H (1997): Revision of the empirical Green's function method by Irikura (1986), Programme and Abstracts. *The Seismological Society of Japan* 2: B25

[10] Ancheta TD, Stewart JP, Abrahamson NA (2011): Engineering characterization of earthquake ground motion coherency and amplitude variability. *4th IASPEI / IAEE International Symposium: Effects of Surface Geology on Seismic Motion August 23-26*, University of California Santa Barbara

[11] Der Kiureghian A, Neuenhofer A (1992): Response spectrum method for multiple support seismic excitation, *Earth. Eng. Struc. Dyn*. 21: 713–740.

[12] Zerva A, Harada T (1997): Effect of surface layer stochasticity on seismic ground motion coherence and strain estimates. *Soil Dynamics and Earthquake Engineering* 16**:** 445-457

[13] Aki K, Richards PG (2002): *Quantitative seismology*, Second Edition, University Science Books, Sausalito, CA

[14] Irikura K (1983): Semi empirical estimation of strong ground motions during large earthquakes. *Bulletin of Disaster Prevention Research Institute*, Kyoto University, Japan 33: 63-104.

[15] Kanamori H, Anderson DL (1975): Theoretical basis of some empirical relations in seismology. *Bull. Seism. Soc.Am*.65: 1073–1095

[16] Kamae K, Bard PY, Irikura K (1998): Prediction of strong ground motion at EURO-SEISTEST site using the empirical Green's function method. *Journal of Seismolgy* 2: 193-207

[17] AfifChaouch K, Tiliouine B, Hammoutene M, Rupakhety, Sigbjörnsson R. (2016): Estimating ground motion incoherence through finite source simulation: a case study of the 1980 El-Asnam Earthquake. *Bull. Earth. Eng*.10: 1193-1204.

[18] Cisternas A, Dorel J, Gaulon R (1982): Models of the complex source of the El-Asnam earthquake. *Bull. Seism. Soc. Am*. 72: 2245-226.

[19] Petrovski J, Milutinovic Z (1981): Deconvolution analysis of surface accelerogram records in El-Asnam region. *Actes des journées scientifiques sur le séisme d'El-Asnam du 10.10.80*, Alger, 15-16 June:373-401

[20] Rupakhety R, Halldorsson B, Sigbjörnsson R (2010): Estimating coseismic deformations from near source strong motion records: methods and case studies. *Bull. Earth. Eng*. 8(4):787—811

[21] Yielding G, Jackson JA, King GCP, Sinvhal H, Vita-Finzi C, Wood RM (1981): Relations between surface deformation, fault geometry, seismicity, and rupture characteristics during the E1-Asnam (Algeria) earthquake of 10 October 1980. *Earth and Planetao Science Letters* 56: 287-304

[22] Dechamps A, Gaudemer Y, Cisternas A (1982): The El-Asnam, Algeria, earthquake of 10 October 1980: multiple-source mechanism determined from long-period records. *Bull. Seism. Soc. Am*. 72: 1111-1128.

[23] Boore DM (1983): Stochastic simulation of high-frequency ground motions based on seismological models of the radiated spectra. *Bull. Seism. Soc. Am*. 73: 1865-1894.

[24] Zerva A (2009): Spatial Variation of Seismic Ground Motions. Modeling and Engineering Applications. CRC Press, Boca Raton.

[25] Rupakhety R, Sigbjörnsson R (2012): Spatial variability of strong ground motion: novel system-based technique applying parametric time series modelling. *Bull. Earth. Eng*.10: 1193-1204.

[26] Jenkins GW, Watts DG (1969): *Spectral Analysis and its Applications*. Holden Day, San Francisco, CA.